LANGMUIR Cite This: Langmuir XXXX, XXX, XXX−XXX

Article

pubs.acs.org/Langmuir

Naphthalimide-Based DNA-Coupled Hybrid Assembly for Sensing Dipicolinic Acid: A Biomarker for *Bacillus anthracis* Spores

Meenakshi Verma,[†] Navneet Kaur,[‡] and Narinder Singh*[,†]

[†]Department of Chemistry, Indian Institute of Technology Ropar, Rupnagar, Punjab, India

[‡]Department of Chemistry, Panjab University, Chandigarh 160014, India

Supporting Information

ABSTRACT: We have designed and synthesized a novel, water-soluble naphthalimide-histidine receptor (**1**) with excellent fluorescent properties. Functioning of the synthesized receptor was performed through developing their DNA−receptor hybrid assembly (DRHA), which has shown significant changes in the emission profile upon interactions with dipicolinic acid (DPA), a biomarker for *Bacillus anthracis* spores. DRHA showed fluorescence enhancement upon binding with DPA with the characteristic of internal charge transfer. It is notable that this assembly exhibited a significant limit of detection (12 nM) toward DPA. The mechanism of sensing was fully defined using ethidium bromide (EtBr) interaction studies as well as Fourier transform infrared spectroscopic analysis, which describes the binding mode of DRHA with DPA. This assembly selectively interacts with DPA over other anions, common cellular cations, and aromatic acids in aqueous media.

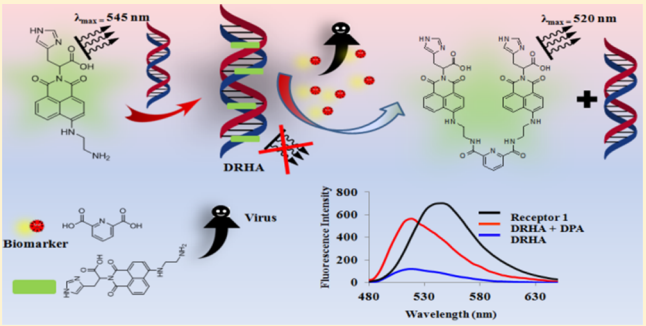

INTRODUCTION

Bacterial contamination in various resources of foodstuff or water necessitates continued development to discover rapid and specific techniques for detecting the pathogens involved.[1] The growth of highly sensitive and selective probes for the recognition and measurement of these pathogens, in vitro, is one of the most necessary tools in biological, chemical, and environmental science.[2] The current scenario leads toward significant progress in the field of biosensors that results in the development of more specific, robust, and economic methods by incorporating emerging variety of techniques from diverse disciplines.[1]

Dipicolinic acid (DPA) is a unique constituent of bacterial spores of *Bacillus anthracis*, accounting for 5−15% of the dry mass of the spores and furthermore is unique to *B. anthracis*. Consequently, DPA plays an important role as a potential biomarker for *B. anthracis*.[3−5] *B. anthracis* is a Gram-positive, rod-shaped, aerobic and facultative anaerobic, and spore-forming bacterium and is one of the most hazardous biological warfare agents because of the possibility of high disaster and mass destruction.[6] This has already been used as a warhead by military and terrorist groups.[7−10] However, its detection is not an easy task, as it takes upto 60 days for anthrax symptoms to appear in humans.[11−13] Therefore, developing a detection method for the biomarker of this infectious agent has been the key point of current research that can work in an environment as well as in the aqueous system. After the anthrax attacks in the United States, the researchers are emphasizing on developing a precise, rapid, real-time, and field-ready detecting system for the same.[14−16] DPA detection, thus, may provide good progression for counting bacteria spore content in the affected material.

Besides the toxicity of bacterial spores, even DPA alone, if inhaled, can lead various systemic or central nervous system effects such as memory difficulties, abnormal fatigue, or dizziness.[17] The present literature reports revealed various biological and chemical techniques to detect DPA through polymerase chain reaction[18−20] and immunoassays;[21,22] however, these are affected with some drawbacks such as prolonged cycles, difficult process, costly reagents, and specialized analysis.[23−26] A list of important chemical methods used for identifying *B. anthracis* includes vibrational spectroscopy [Fourier transform infrared (FTIR), Raman, and surface-enhanced Raman],[27−31] capillary zone electrophoresis,[32] potentiometric sensors,[33] high performance-liquid chromatography,[34] and pyrolysis mass spectrometry,[35] and optical detection. The optical methods/luminescence techniques have currently attracted the interest of the researchers, as these are rapid, highly sensitive and selective, and economically viable and offer easy operation.[36−41]

In general, optical sensing of bacterial spores is based on the detection of DPA and is a major component of *Bacillus* spores.[42] It is evident from literature reports that the lanthanides showed good potential for DPA detection because of their distinctive and quick complexation with DPA.

Received: January 31, 2018
Revised: March 26, 2018

DOI: 10.1021/acs.langmuir.8b00340
Langmuir XXXX, XXX, XXX−XXX

Scheme 1. Synthesis Scheme of Receptor 1

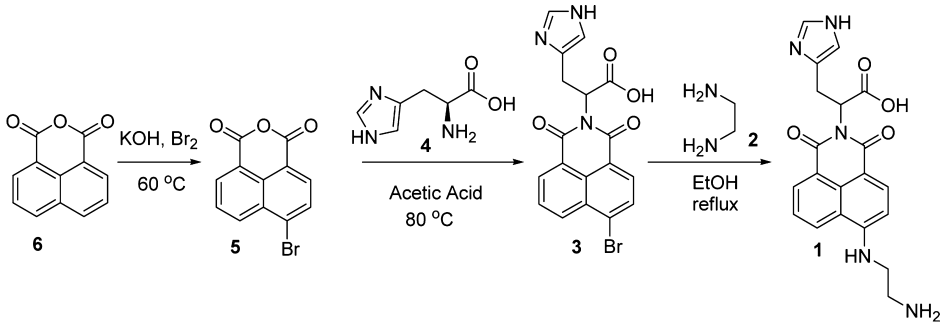

However, as per reports, the fluorescence intensity of lanthanides is recognized to be responsive to external conditions, for example, the preparation method, apparatus setup parameters, ionic concentration, and the nature of target moiety.[26,43] Consequently, it becomes the need of the hour to find some alternatives to overcome these drawbacks. Herein, we report a naphthalimide-based DNA receptor hybrid assembly (DRHA) for detection of DPA. Naphthalamide is the fluorophore tag of choice because of its outstanding photophysical properties that include high extinction coefficient, photostability, and relatively long emission wavelength.[44] The strong emission character of 1,8-naphthalimide derivatives in organic and aqueous media is thought to be due to their internal charge-transfer (ICT) excited-state transition.[45]

1,8-Naphthalimide derivatives having an aromatic core moiety and bearing a basic side chain offer good DNA binding affinity either by intercalation or groove binding. The synthetic strategy allows modifications with a variety of functional groups on both sides: the aromatic "naphthalene" moiety and the "N-imide site".[46,47] The carbonyl group of naphthalimide has an electron-withdrawing nature and hence facilitates the introduction of electron-donating groups (e.g., amines) in the molecular design.[48] The presence of an electron-donating amine group in the 3- or 4-position provides a green-emitting fluorophore with tremendous photochemical stability and good quantum yields.[45] A system containing naphthalimide as its core molecule has been used tremendously not only as colorimetric and luminescent[45] sensors for ions and biomolecules but also in cellular imaging applications[11] and generation of fascinating supramolecular assemblies.[49] These derivatives have also been used in numerous other applications, for example, as luminescent probes for selective staining of live cells, stimuli-responsive hydrogels, and in photochemical welding of tissues.[45] Interestingly, their properties are extendable as tunable dye lasers, polymerizable materials, and electroluminescent organic diodes in thin films.[50]

In the present work, the structure design utilized the structural benefits of naphthalimides, and the synthesized assembly is also appended with the following: (a) histidine moiety that possibly offers solubility in aqueous media and (b) the aliphatic amine group owing to its good binding capabilities. In comparison to the previously known DPA sensors, the naphthalimide-based optical sensor seems more lucrative owing to its fluorescence properties and ease of use.[26] To the best of our knowledge, this is the first report in which the naphthtalimide-based probe is used as the optical detector against DPA. The developed DRHA has shown an active response in an aqueous medium; therefore, the practical utility of DRHA toward DPA has been investigated in tap water, canal water, and rainwater.

EXPERIMENTAL SECTION

General Information. 1,8-Naphthalic anhydride, bromine, L-histidine, and ethylenediamine were purchased from Sigma-Aldrich/local suppliers and were used without further purification. Milli-Q water (18.2 MΩ·cm at 25 °C) was used to prepare all aqueous solutions. Purified solvents of commercial grade were purchased from Loba, Spectrochemicals, and Aldrich. The ^{1}H NMR and ^{13}C NMR spectra were recorded on the Jeol Instrument working at 400 MHz for ^{1}H NMR and at 100 MHz for ^{13}C NMR. All chemical shifts were recorded in ppm relative to tetramethylsilane as an internal reference. The UV−vis absorption spectra were recorded on a Shimadzu 2400 spectrophotometer using cuvettes of 1 cm path length. The fluorescence experiments were conducted at room temperature on a PerkinElmer LS-55 Spectrophotometer with a fixed scanning speed and emission slit width (10 nm). Particle size was determined by dynamic light scattering (DLS) using the external probe feature of the Metrohm Microtrac Ultra Nanotrac particle size analyzer. Time-resolved fluorescence decay studies were performed on a PicoQuant FluoTime 300 high-performance fluorescence lifetime spectrometer. FTIR spectra images were obtained using a Bruker photospectrometer. Circular dichorism (CD) spectra were recorded on a JASCO, J-1500 circular dichroism spectrophotometer between 400 and 200 nm in the continuous scanning mode (200 nm/min).

Synthesis and Characterization of 3. The bromination of 1,8-naphthalic anhydride (**6**) was achieved as per the method described in the literature.[51,52] Briefly, to a solution of 1,8-naphthalic anhydride (1.98 g, 10.0 mmol) in KOH (2.8 g in 12 mL water), 2 mL of bromine was added drop-wise at room temperature. The reaction mixture was stirred at room temperature for 30 min and then heated to 60 °C for 6 h. On the completion of the reaction, light brown colored precipitates separated out. The reaction mixture was acidified with concentrated hydrochloric acid (HCl), and the solid residue was then filtered. The crude product was further heated with 5% NaOH solution and filtered, and the filtrate was neutralized with HCl solution. Solid precipitates separated out which were filtered and washed with cold water and dried to get yellow-brown powder of 4-bromo-1,8-naphthalic anhydride (**5**). To synthesize **3**, compound **5** (2.77 g, 10 mmol) was suspended in acetic acid, and then L-histidine (1.55 g, 10 mmol) was added to it. The resulting solution was then heated to 80 °C for 8 h and cooled to room temperature after completion of the reaction. Ice cooled water was added to this solution and filtered to get dark brown solid of the compound **3** which was washed with water a number of times to get rid of any trace amounts of acetic acid. Yield = 82%. mp = 183−185 °C. ^{1}H NMR (400 MHz, DMSO-d_6): δ 8.55 (t, J = 8 Hz, 2H, ArH), 8.29 (d, J = 8 Hz, 1H, ArH), 8.20 (d, J = 8 Hz, 1H, ArH), 7.99 (t, J = 8 Hz, 1H, ArH), 7.34 (s, 1H, His-ArH), 6.65 (s, 1H, His-ArH), 5.73 (m, 1H, His-CH), 3.41 (m, 2H, His-CH_2). ^{13}C NMR (100 MHz, DMSO-d_6): δ 171.13, 163.01, 135.22, 133.53, 132.59, 132.07, 131.96, 130.37, 130.09, 129.52, 128.75, 122.79, 117.37, 54.09, 26.30. Anal. Calcd for $C_{18}H_{12}BrN_3O_4$: C, 52.19; H, 2.95; Br, 19.24; N, 10.19;

DOI: 10.1021/acs.langmuir.8b00340
Langmuir XXXX, XXX, XXX−XXX

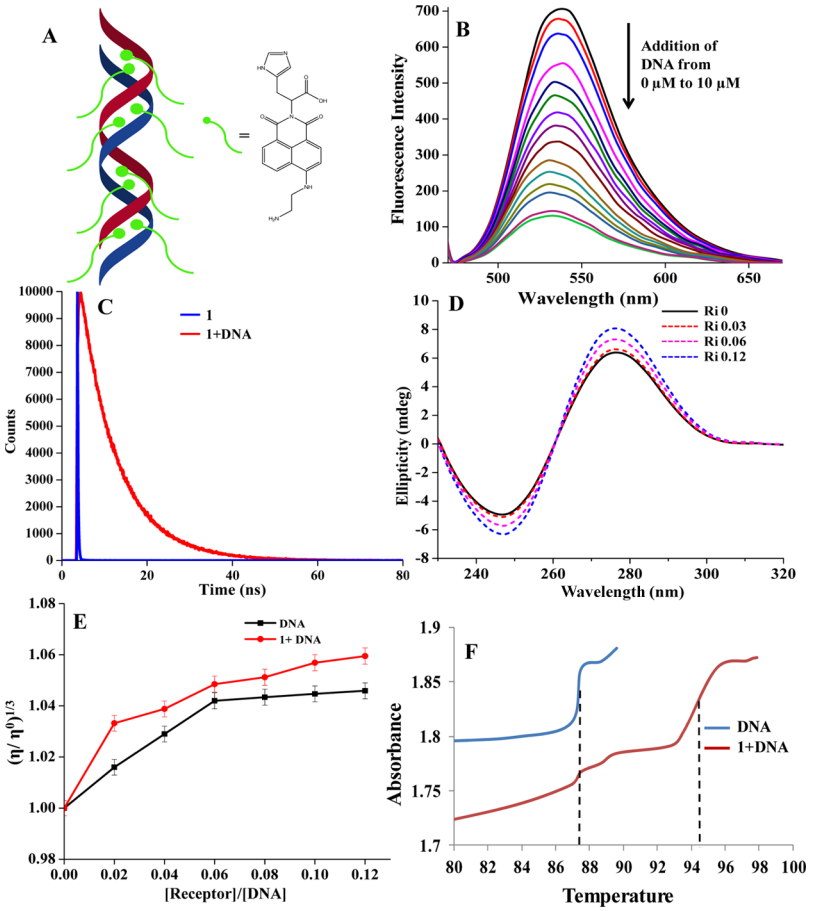

Figure 1. (A) Schematic diagram showing the interaction of organic receptor **1**; (B) changes in fluorescence intensity of receptor **1** (1 μM) upon the successive addition of DNA (0−10 μM) in aqueous medium (λ_{ex} = 460 nm); (C) typical time-resolved fluorescence decay profile of receptor **1** and the same receptor in the presence of 10 μM salmon sperm DNA; and (D) circular dichroism (CD) spectra of salmon sperm DNA incubated 18 h with receptor **1** at different [receptor]/[DNA] ratios at 37 °C. (E) Effect of the increasing concentration of receptor **1** on the relative viscosity of salmon sperm DNA at 25 °C. (F) Variation in melting temperature of DNA on the addition of receptor **1**.

O, 15.40. Found: C, 52.23; H, 2.95; Br, 19.24; N, 10.19; O, 15.40. MS (EI): m/z 414.07 (M^+ + 1).

Synthesis and Characterization of 1. Compound **3** (0.413 g, 1 mmol) was refluxed overnight with ethylenediamine (**2**) (10 mmol) using ethanol as the reaction solvent. Reaction was monitored with thin-layer chromatography (TLC) and on completion of reaction, the solvent was evaporated under vacuum. The crude product was then purified using column chromatography and collected as a yellow solid. Yield = 85%. mp = 169−171 °C; FT-IR ν: 2981, 2939, 2831, 2252, 1705, 1640, 1527, 1350, 1172, 1107, 1014, 948 cm^{-1}. ^1H NMR (400 MHz, DMSO-d_6): δ 8.47 (d, J = 12 Hz, 2H, ArH), 8.24 (m, 1H, ArH), 8.15 (d, J = 8 Hz, 1H, ArH), 7.93 (t, J = 8 Hz, 1H, ArH), 7.30 (d, J = 8, 1H, His-ArH), 6.47 (d, J = 12 Hz, 1H, His-ArH), 5.45 (m, 1H, His-CH), 3.49 (m, 2H, His-CH_2), 3.37 (m, 2H, −CH_2), 3.25 (t, d = 12 Hz, 2H, −CH_2). ^{13}C NMR (100 MHz, DMSO-d_6): δ 163.12, 134.91, 134.73, 132.93, 132.33, 132.10, 131.91, 131.52, 130.26, 129.36, 128.73, 79.72, 56.58, 26.88, 23.31. Anal. Calcd for $C_{20}H_{19}N_5O_4$: C, 61.06; H, 4.87; N, 17.80; O, 16.27. Found: C, 61.11; H, 4.81; N, 17.85; O, 16.23. MS (EI): m/z 394.21 (M^+ + 1).

Intercalation of the Receptor with DNA. The solution of receptor **1** was prepared at 1 mM concentration in water and sonicated well before recording the spectra. Receptor **1** was freely soluble in water, and hence, all binding studies were performed at pH 7.5 using HEPES buffer. A stock solution of salmon sperm DNA was prepared by dissolving DNA in phosphate buffer. Absorption spectroscopic changes were observed by adding DNA in incremental amounts (0−10 μM) to the fixed amounts of the receptor (1 μM). The fluorescence changes were observed with the incremental addition of DNA (0−10 μM) to the fixed amounts of the receptor (1 mL). The fluorescence measurements were performed, maintaining the excitation and emission band slit width of 10 nm. A fluorescence-free quartz cell of 1 cm path length was used. CD spectra of DNA alone and in the presence of receptor **1** were recorded at room temperature in the wavelength range of 200−700 nm, at different compound/DNA ratios, however, keeping the DNA concentration constant. The optical chamber of the CD spectrometer was deoxygenated with dry nitrogen, and samples were held under nitrogen atmosphere during the measurements. Viscosity measurements were carried out using Ostwald's viscometer suspended vertically in a thermostat at 25 °C. The flow time was measured with a digital stopwatch, and the sample was tested three times to get an average calculated time. Data obtained were plotted as $(\eta/\eta^0)^{1/3}$ versus [compound]/[DNA] ratio, where η and η^0 denote the specific viscosity of salmon sperm DNA in the presence and absence of the receptor **1**, respectively, and their values were calculated using formula $(t - t_b)/t_b$, where t denotes the observed flow time in the presence of receptor **1** and t_b stands for the flow time of buffer alone.[53,54] DNA melting experiments were carried out by observing the absorbance of salmom sperm DNA at 280 nm at various temperatures in the absence and presence of testing receptor **1** with a ramp rate of 1 °C/min in a phosphate buffer (pH 7.0) on a Shimadzu spectrophotometer equipped with a Peltier thermoregulator. The transition midpoint of the melting curve was assigned as T_m. The particle size of aggregates of receptor **1** alone as well as in the presence of DNA was determined with DLS using the external probe feature of the Metrohm Microtrac Ultra Nanotrac particle size analyzer. The data revealed that the particle size lies in the μm range.

DOI: 10.1021/acs.langmuir.8b00340
Langmuir XXXX, XXX, XXX−XXX

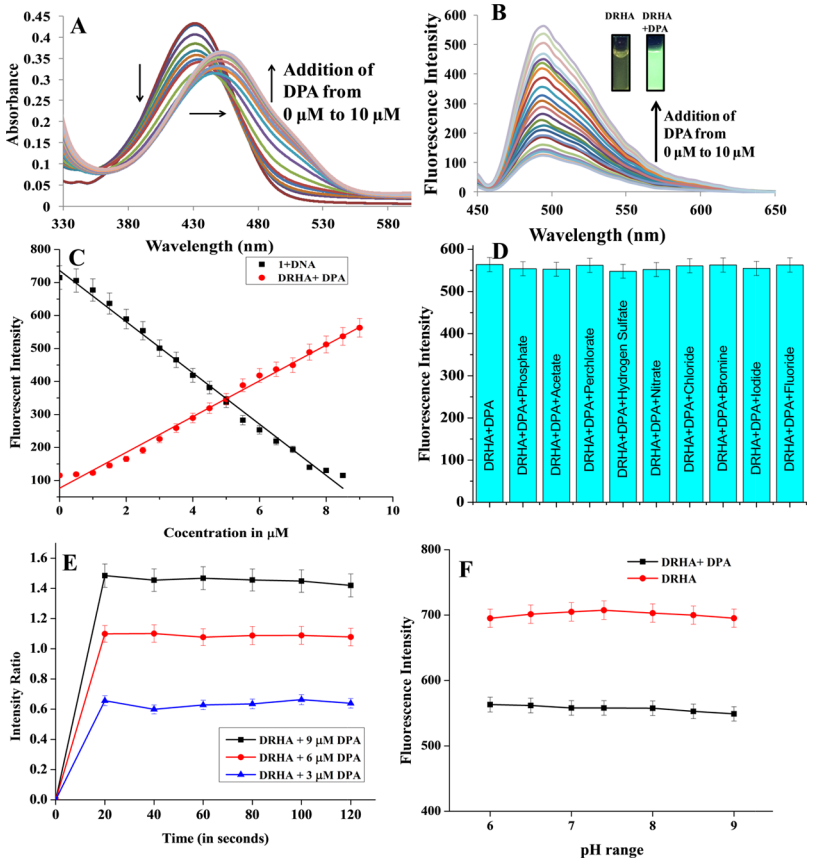

Figure 2. Recognition of DPA with DNA–receptor hybrid assembly (DRHA): (A) changes in absorption spectra of DRHA upon the successive addition of DPA (0–10 μM) in aqueous medium; (B) changes in the fluorescence intensity of DRHA upon the successive addition of DPA (0–10 μM) in aqueous medium (λ_{ex} = 430 nm), and emission from solution under UV light is shown in the inset of the figure (inset); (C) linear regression graph between concentrations of DNA added to receptor **1** (decrease in fluorescent intensity) and concentrations of DPA added to DRHA (increase in fluorescent intensity); (D) competitive binding studies of DRHA containing DPA over other selected anions; (E) plot of the intensity ratio of DRHA and DPA at different concentrations as a function of time in seconds; (F) effect of pH on DRHA (1 μM) alone and in the presence of DPA in an aqueous system.

DPA Recognition Using DRHA. The DRHA was used to recognize DPA (dipicolonic acid). The solution of organic receptor **1** was prepared at 1 mM concentration in the buffer and sonicated well before recording the spectra. All binding studies were performed at pH 7.5 using HEPES buffer. The stock solutions of DNA and DPA were prepared at a concentration of 1 mM (pH 7.5, HEPES buffer). The real sample analysis experiment was based on evaluating the functioning of the sensor in various environmental samples. For this, water samples from various sources were collected. To calculate the detection limit, a graph was plotted between the concentration and the fluorescence intensity. The detection limit was calculated by using the formula: DL = (3 × SD)/m.

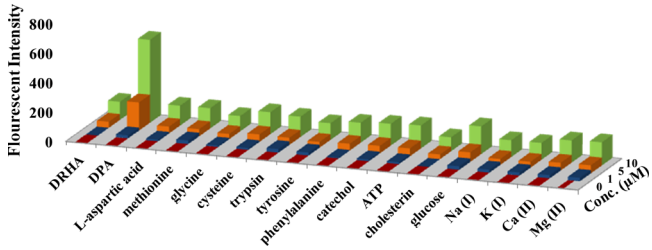

Figure 3. Selectivity test of DRHA for DPA: detection over several amino acids, aromatic ligands, and cellular cations. The concentrations of all the compounds are the same, and measurements are performed under identical conditions.

RESULTS AND DISCUSSION

Synthesis and Characterization of the Receptor. Receptor **1** has been designed to target the recognition properties for the desired analyte, and the receptor design is fabricated with the histidine group that may impart the water solubility to the receptor and the naphthalimide unit as fluorescent signaling subunits. The naphthalimide unit is articulated with the amine group for binding with the biomarker, and it is envisioned that once the biomarker binds with the $-NH_2$ group, this binding event will modulate the fluorescence signature of the naphthalimide moiety. The synthesis of the desired receptor was achieved through the bromination of 1,8-naphthalic anhydride using a method reported in the literature.[51,52] Compound **3** was synthesized by reacting **5** with 1 equivalent of L-histidine in acetic acid. After 8 h of heating at 80 °C, the reaction mixture was cooled to room temperature, which yielded the precipitates. The precipitates were filtered and washed with an excess of water to remove any traces of acetic acid. In next step, the target receptor **1** was synthesized by reacting compound **3** with an excess of ethylenediamine in ethanol under reflux. The progress of the reaction was monitored with TLC, and upon completion of reaction, the crude product was purified using column chromatography. Spectroscopic data confirmed the formation of receptor **1** (Figures S1–7).

DOI: 10.1021/acs.langmuir.8b00340
Langmuir XXXX, XXX, XXX–XXX

Table 1. Analysis of Spiked Samples of DPA in Real Water Samples (n = 3) Using Synthesized DRHA[ab]

	DPA added (nM)	DPA found (nM)	% recovery
tap water	0	N.D.	0
	20	18.13 ± 0.05	95.65
	40	38.91 ± 0.05	97.27
canal water	0	N.D.	0
	20	18.85 ± 0.05	94.25
	40	37.57 ± 0.05	93.92
rain water	0	N.D.	0
	20	18.41 ± 0.05	92.05
	40	38.46 ± 0.05	96.15

[a]Recovery = (amount found in the spike sample − amount found in the original sample) × 100/amount added. [b]N.D.: not detected.

Table 2. Intraday and Interday Precision and Accuracy of Analytes (n = 4)

nominal concentration (nM)	measured average concentration (nM)	SD	RSD %	relative error %
	Intraday Assay			
20	18.24	0.76	4.21	1.18
40	36.72	1.39	3.80	1.31
60	56.25	1.57	2.79	1.78
80	74.45	1.96	2.63	1.89
	Inter-Day Assay			
20	17.24	0.78	4.53	1.10
40	36.32	1.04	2.87	1.74
60	54.65	1.70	3.11	1.60
80	73.95	1.43	1.94	2.57

Intercalation of the Receptor with DNA. The synthesized organic receptor (**1**) was tested for its binding affinity with DPA (10 μM) through the modulation of absorption and fluorescence signatures of **1** with respect to the varied concentrations of DPA. However, contrary to our expectation, insignificant changes were detected in absorption and emission spectra of the receptor **1** upon the addition of DPA. The most probable reason expected is the hindrance of amide bond formation between the receptor **1** and DPA. However, the recent account of Silverman revealed that such bond formation can be modulated in the presence of DNA.[55] Thus, in the present work, we decided first to understand the intercalation of receptor **1** with DNA, and eventually, the DRHA will be used to sense the biomarker. To explore the binding mode of DNA with receptor **1**, various studies have been performed, and these studies proposed the intercalating nature of receptor **1** with DNA. Figure 1A presents the schematic diagram showing the interaction of the organic receptor with DNA. To support this intercalation, spectroscopic analysis was performed, where the UV−vis absorption spectroscopy has provided important information on the mode of binding of molecules to DNA. The addition of salmon sperm DNA (5 equiv) to the solution of **1** (1 mL) showed modulation in the absorbance and emission profile of the receptor **1**. To examine the binding approach between DNA and receptor **1**, titrations were carried out in which the concentration of the receptor was kept constant (1 mL) and the DNA concentration was varied from 0 to 10 μM and the titrations were monitored with UV−vis absorption spectroscopy. Upon the incremental addition of DNA, the hypochromic shift has been observed without any band shift in the absorption spectra of **1** (Figure S8). The observed "hypochromic" spectral changes suggested that receptor **1** exhibited good binding tendency for salmon sperm DNA. It is a well-known fact in the literature that hypochromism is a characteristic property of intercalating molecules.[56,57] Further, the extent of the hypochromism is related to the strength of intercalative interaction, where this mode of binding comprises the stacking interaction between an aromatic chromophore and the base pair of DNA. Fluorescence spectroscopy is one of the most precise methods for studying the comparative binding of

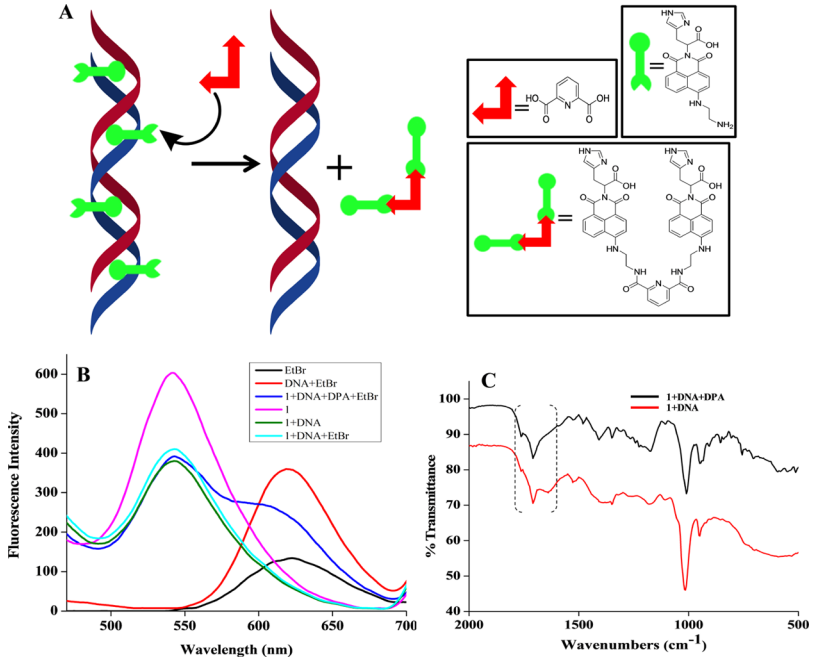

Figure 4. (A) Diagrammatic representation of the mechanism of sensing of DPA with DRHA; (B) ethidium−bromide interaction experiment showing interactions between DRHA and DPA; and (C) IR spectra of DRHA alone and in the presence of DPA.

DOI: 10.1021/acs.langmuir.8b00340
Langmuir XXXX, XXX, XXX−XXX

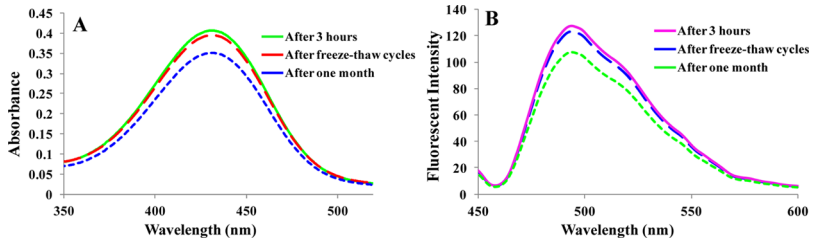

Figure 5. (A) Absorption and (B) emission spectra of DRHA showing its short-term, freeze−thaw, and long-term stability.

Table 3. Comparison of the Limit of Detection of Fluorescent Sensors for the Detection of DPA as a Biomarker of *B. anthracis*[a]

fluorescent sensor	linear	LODs	detection in water	real sample analysis	interference	ref
Eu−GNPs		1 μM				72
Tb−GNPs						
Eu−PVA film	non-linear	100 nM	yes	yes	no interference	66
Tb−silica NPs		56.6 nM			no interference	64
Tb/Eu@bio-MOF		34 nM	yes	yes	no interference	73
Tb−polymer	0−20 μM	10 nM	yes		no interference	68
FA:Tb−EDTA		8.2 nM		yes	no interference	69
FA:Eu−EDTA		20.9 nM				
AgNPs−Tb	40 nM to 10 μM	6.7 nM	yes	yes	no interference	70
Tb/Eu−MOFs	50−700 nM	4.55 nM	yes	yes	no interference	26
Tb−CDs	0.005−1.2 μM	5 nM	yes		no interference	71
CDs	0.25−20 μM	79 nM	yes	yes	no interference	65
DRHA	0−9.5 μM	12 nM	yes	yes	no interference	this work

[a]MOFs: metal−organic frameworks. GNPs: gold nanoparticles.

small molecules to DNA as fluorescence quenching measurements can be used to evaluate binding.[18,51] The interaction between receptor **1** and salmon sperm DNA in an intercalation mode causes a strong fluorescence quenching. Receptor **1** with λ_{max} = 545 nm (λ_{ex} = 460 nm) showed quenching with the successive addition of DNA (0−10 μM) (Figure 1B). The time-resolved fluorescence decay behavior has been monitored under differential circumstances to achieve a deeper insight into the photophysical properties of receptor **1** and its modulation in the presence of DNA. The fluorescence lifetime indicates the average time of the excited state of any molecule in its excited state.[58] Figure 1C represents the time-resolved fluorescence decay profile of receptor **1** under varied experimental conditions. The results revealed a single exponential decay for receptor **1** emissions, and the lifetime was found to be 4.7 ns. However, the receptor intercalated with DNA revealed that the decay was at 4.26 and 2.08 ns and hence offers a biexponential response. It confirms energy transfers in the excited state and could be static or dynamic.[59] CD is another technique used to expose the changes in the DNA conformation during molecule−DNA interactions.[60] To confirm whether the synthesized receptor is capable of inducing DNA conformational changes, CD measurements were recorded in the 200−500 nm range. The DNA concentration was kept constant during the experiment, while that of the receptor kept on changing. The CD spectrum of salmon sperm DNA has two bands, the negative band at ∼245 nm (helicity) and a positive band at ∼275 nm (base stacking). These bands in the CD spectrum emanate from the base stacking interactions and the double helical supra structure of the polynucleotide, thereby providing asymmetric environments for the nucleobases.[53] Simple groove binding or electrostatic interactions of DNA and receptor result in slight perturbation of the original CD profile of DNA. However, an intercalating molecule enhances the intensity of both bands owing to disturbance of the stacking of the nucleobases on intercalation.[53] Upon the addition of receptor **1** to salmon sperm DNA, the CD spectrum shows increase in intensities of both the positive and negative bands, proposing that this receptor binds with DNA through intercalation (Figure 1D).[61] The viscosity experiment is a useful tool to detect binding modes between DNA and small molecules, which is generally performed to clarify the mode of binding. Ethidium bromide, being one of the well-known DNA intercalators, causes the DNA helix to increase its length by separating its base pairs to adjust itself, resulting in net viscosity increase.[55,56] Though a compound that attaches electrostatically via the sugar-phosphate backbone generates bends in the DNA helix which reduce its effective length and hence change its viscosity, DNA groove binding under the same experimental environment usually results in little or no effect on DNA viscosity.[56,57] To know the type of binding between synthesized receptor and DNA, viscosity measurements has also been executed using the Ostwald viscometer. The experiments were conducted by adding appropriate amounts (0−120 μM) of receptor **1** into the viscometer to give a particular ratio (r = [receptor]/[DNA]), while keeping the salmon sperm DNA concentration constant. The flow time was determined using a digital stopwatch, and the mean values of three independent measurements were used to evaluate the average relative viscosity of the sample.

Plots of obtained data are represented as $(\eta/\eta^0)^{1/3}$ versus [receptor]/[DNA] ratio, where η^0 and η are the specific viscosity of salmon sperm DNA in the presence and absence of the receptor **1**, respectively. Relative viscosities of salmon sperm DNA were calculated from (η/η^0).[54] The data shown in Figure 1E exhibited a notable change in relative specific viscosity, indicating intercalative binding of receptor **1** toward salmon sperm DNA. Further, the high temperature can destroy

DOI: 10.1021/acs.langmuir.8b00340
Langmuir XXXX, XXX, XXX−XXX

the double helix structure of DNA and transform it into a single helix at the melting temperature (T_m). Interaction of small molecules with DNA can affect the melting temperature by increasing it about 5−8 °C,[62] which can be justified on the basis of intercalation binding that provides extra stability to the DNA helix. Nonintercalative bindings do not show such an effect. DNA melting studies further support the DNA intercalating nature of receptor **1**. The interactions of synthesized receptor **1** with salmon sperm DNA were determined through thermal denaturation experiments. The value of T_m was changed to a notable extent. For pure salmon sperm DNA, the melting temperature is 87.5 °C which increased to 94.3 °C upon the addition of receptor **1**. This supports the fact that the interaction between DNA and receptor **1** is intercalative (Figure 1F). The particle size of aggregates of receptor **1** has been determined from DLS histograms, and it has been found that the size of aggregates of **1** is 0.57 μM. The effect of the addition of a fixed amount of DNA on the size of these aggregates has also been determined. The size increased from 0.57 to 0.66 μm. It can be concluded that the size increase on the addition of DNA to the host receptor is due to aggregation (Figure S9).

DPA Recognition Using DRHA. To evaluate the recognition profile of the DRHA, it was exposed to different concentrations of DPA in an aqueous solution and absorption, and the emission profile of the solutions has been tested against the increasing amount of DPA (0−10 μM). The absorption spectra of DRHA showed an absorbance band at 430 nm, which shifted to 451 nm on the addition of 10 μM of DPA. The titration between DRHA and DPA showed a distinctive trend when the titration was monitored with UV−vis absorption spectroscopy. With the increasing concentration of DPA, the absorbance band showed hypochromic as well as bathochromic shift up to 445 nm. Beyond this, the band showed an upward shift along with bathochromic (Figure 2A). This response is well-explored for the intramolecular charge transfer (CT) behavior of naphthalimide-based moieties which are widely used in fields such as sensing, intracellular biomarkers, or fluorescence imaging.[63] Fluorescence titrations have also been performed to confirm the binding capability of DRHA with DPA. The successive addition of a standard amount of DPA showed enhancement in the emission band at 520 nm (λ_{ex} = 430 nm). The emission changes on the addition of DPA are noticeable under UV light (inset Figure 2B). DRHA shows evident emission spectra change on the addition of DPA. Fluorescence intensities gradually increased with increasing amounts of DPA. As shown in Figures 2C and S11, the concentration of the DPA measurements can be linearly correlated well with the fluorescence intensity values in the 0−9 μM concentration range with a correlation coefficient of 0.9933. Using the linear response, a calibration curve can be constructed, which can then be used to determine the amount of DPA in an unknown sample quantitatively.[64] Such a sensitivity of the DPA sensor does not require any additional calibration of the fluorescence intensity. The limit of detection (LOD) of this sensor can be defined as $3 \times SD/m$, where SD is the standard deviation and m is the slope of the working curve. The detection limit of DRHA for DPA is obtained to be 12 nM, which is much less than the magnitude of an infectious dose of the spores for human beings (60 mM).[65]

To evaluate the selectivity of the sensor, competitive binding studies were carried out, where the host solution of DRHA (1 μM) was taken in different nine volumetric flasks, and then 1 μM of DPA solution was added to each flask. Tetrabutylammonium anion salts (PO_4^{3-}, CH_3COO^-, ClO_4^-, HSO_4^-, NO_3^-, Cl^-, Br^-, I^-, F^-) were used as potential interference entities as the DPA is dicarboxylate and with the modulation of pH, it may offer the anionic species. Each solution was kept for equilibrium, these solutions were shaken after a regular time interval, and finally, the fluorescence measurements were performed with each solution independently. Comparison of fluorescence spectra of DRHA + DPA alone and of DRHA + DPA in the presence of various anions showed that there is no interference from the other anions and the sensor is highly selective for DPA (Figure 2D).

Although the sensor has offered high selectivity, sensitivity is another important criterion for the successful operation of the sensor: short response time is mandatory for a sensor meant for real-time applications. To study the response time of DRHA for sensing of DPA, the fluorescence spectra were recorded with solutions containing different concentrations of DPA (3.0, 6.0, and 9.0 μM) to the solutions of DRHA (1.0 μM), and each solution was analyzed as a function of time. The response time of DRHA to detect DPA is concentration-independent, as the time required to reach equilibrium does not affect DPA concentrations. The interpretation of results revealed that after 60 s, the fluorescence intensity of all three solutions is independent of time; in other words, the response time of DRHA for DPA is less than 60 s (Figure 2E). To gain more insights about the application of the sensor, the performance of the fluorescent sensor for target moiety was evaluated under varied pH conditions. This was evaluated by monitoring the effect of pH on the fluorescence response of DRHA and DRHA + DPA. During these studies, both acidic and basic titrations were conducted by changing pH of DRHA and DRHA + DPA solutions independently using sodium hydroxide/hydrochloric acid. The pH window ranging from 6.0−9.0 for DRHA and DRHA + DPA both were found to be best for the operation of the sensor (Figure 2F).

To investigate the selective utility of DRHA, we further performed competitive binding assay: a number of possible interference moieties have been selected including glycine, L-aspartic acid, methionine, cysteine, trypsin, tyrosine, and phenylalanine as representative amino acids as well as a collection of different competitive protic/bidentate substrates/aromatic acids (e.g., catechol, adenosine triphosphate, cholesterin, glucose, benzoic acid, 2-picolinic acid, 3-aminobenzoic acid, 2,6-dihydroxy benzoic acid, isophthalic acid, *p*-toluic acid, and nicotinic acid) and analyzed these results against those of DPA (Figures 3 and S10). In addition, various common cellular cations (Na^+, K^+, Ca^{2+}, and Mg^{2+}) (Figure 3) were also tested along with anions (Figure 2D). All or a number of this interference may be the constituent of bacterial spores.[66] This study revealed that some biologically or structurally relevant small molecule analytes have a slight or negligible effect on the emission profile of DRHA as compared to DPA. It can be seen that only DPA induces a prominent fluorescence enhancement in the DRHA fluorescence profile at various concentrations, concluding excellent selectivity of DRHA for DPA, which may facilitate the recognition of this anthrax biomarker in a complex environment.

The abovementioned results conclude that DRHA has good practical applicability for environmental applications and has no effect on the other environmental analytes present in water. Finally, the workability of the proposed DRHA was tested for the determination of DPA in real samples collected from

DOI: 10.1021/acs.langmuir.8b00340
Langmuir XXXX, XXX, XXX−XXX

different sources (tap water, canal water, and rain water). To establish the practical application, water samples were filtered through a syringe filter to eliminate any biological impurity. Now, the known concentrations of DPA (0, 20, and 40 nM) have been pierced into the samples and tested against the developed sensor. To check practical workability of the synthesized sensor in real sample analysis, these samples were subjected to analysis using proposed DRHA. The results are shown in Table 1. It is clear from the results obtained that the proposed assembly was able to determine the DPA concentrations in these samples with a good precision value.

The ICT-based naphthalimide derivatives have been the most accepted preference in chemosensors among all. The reason behind its popularity is that it strongly absorbs and emits at long wavelengths, which is highly desirable for sensing in competitive media.[67] Herein, a mechanism has been proposed for binding of DRHA and DPA. The absorption and emission changes are a result of CT interactions between the donor and the acceptor. It is a well-known fact that the reaction of the sensor with the interacting molecule switches on the ICT process and induces an emission shift. Our approach to fluorescence detection of DPA relies on ICT within the DRHA platform. The electron-donating amino group on the organic receptor affects both ICT and the emission profile, as making the substituent more electron-deficient results in ICT-induced hyperchromic shifts in emission maxima. Figure 4A demonstrates the diagrammatic mechanism of recognition of DPA.

In support of this approach, ethidium bromide−DNA interaction studies were carried out. Ethidium bromide (EtBr) was added to a sample containing 10 μM of DRHA. It was observed that the emission band at 545 nm remained undisturbed, showing the insignificant effect of the addition of EtBr on the emission spectra. In next step, to confirm the interactions between DRHA and DPA, first DPA was added to DRHA, and the solution was shaken properly. Then, EtBr solution was added.

A new band was observed to appear near 610 nm typically because of the EtBr/DNA complex formation (Figure 4B). It supports the fact that the amino group of receptor **1** reacts with DPA, leaving behind the DNA undisturbed. It reveals the information that the amino group of receptor **1** reacts with DPA, leaving the DNA undisturbed. A variation in IR spectra of DRHA (in the absence and presence of DPA) near 1600 cm^{-1} also confirms the interactive nature of the amino group and DPA (Figure 4C).

Statistical Analysis. *Limit of Quantification (LOQ) and LOD.* The LOD and LOQ values were calculated from duplicate measurements for each concentration of DPA. The LOQ and the LOD for DPA were determined by multiplying the standard error of the *y*-intercept by 10 and 3, respectively, and dividing these values by the slope of the calibration curve. The LOQ and LOD were determined to be 12 and 18 nM, respectively.

Precision and Accuracy. Precision is a measure of the reproducibility of the complete analytical process including sample preparation and analysis under normal operating conditions. The results concerning the accuracy and intra- and interday precision of the method have been shown in Table 2 for different concentration levels of DPA. Precision was determined using the method to analyze a 20, 40, 60, and 80 nM DPA standard 10 times and then exhibiting the precision as the relative standard deviation. The intra- and interday precision values were less than 4.21 and 4.53%, respectively, and the relative error was between 1.10 and 2.57%, which indicated the acceptable accuracy and precision of the developed assembly. Also, we performed the binding studies of different batches of DRHA toward DPA. The obtained result showed the same trend for all. It reveals that DRHA is a reliable and reproducible sensing assembly for the detection of DPA.

Stability and Temperature Effects. The stability of synthesized assembly was established under three conditions:

1. Freeze−thaw stability: after going through three freeze−thaw cycles (from −20 °C to room temperature)
2. Short-term stability: at room temperature for the time of regular work (at least 3 h)
3. Long-term stability: in stock solutions at storage conditions (−20 °C) for 1 month.

To ensure the reliability of results and handling/storing of the synthesized assembly, stability studies were carried out. In each situation, deviations from the original values were less than ±5%. As shown in Tables S1 and S2, the synthesized assembly was found to be stable for 3 h at ambient temperatures, after three freeze−thaw cycles and storage for 1 month at −20 °C. These results revealed that no spontaneous degradation was found during the routine sample analysis and storage. Further, absorption and emission spectra of DRHA were recorded after 3 h, freeze−thaw cycles, and after one month to check its short-term and long-term stability. Both, the absorption and emission spectra (Figure 5A,B) showed insignificant change in the original values, which supported the stability of the system.

Comparison of the LOD of DRHA with Reported DPA Sensors in the Literature. The performance and functioning of the synthesized assembly for detection of DPA were also compared with the previously reported lanthanide-based/ratiometric fluorescent sensors. As is compared in Table 3, the LOD acquired using synthesized assembly was comparable to some of the previously reported sensors,[68−70] a little more than three of them,[26,71,72] while showing much lower value than others[64−66,72,73] (Table 3). As is clear from the literature, the LOD obtained (12 nM) by DRHA is lower than the characteristic infectious dosage of *B. anthracis* spores (60 mM)[65] for human beings. Moreover, the synthesized assembly attains full advantage of water-soluble, good fluorescence properties, including fast response, good precision and accuracy, and stability over a good temperature range.

CONCLUSIONS

In conclusion, a naphthalimide-histidine receptor was synthesized using the multistep reaction scheme. The fluorescent organic receptor was then modified by the formation of its DNA hybrid. Various techniques such as CD spectroscopy, viscosity measurements, DNA denaturation experiments, DLS studies, and time-resolved fluorescence studies have been done to explore the DNA−receptor binding nature. The resulting DRHA was used to detect DPA in an aqueous system with an LOD of 12 nM. Response time studies exhibited quick binding of the proposed assembly with DPA. Real sample analysis confirmed the practical applicability of the probe for environmental applications.

ASSOCIATED CONTENT

Supporting Information

The Supporting Information is available free of charge on the ACS Publications website at DOI: 10.1021/acs.langmuir.8b00340.

DOI: 10.1021/acs.langmuir.8b00340
Langmuir XXXX, XXX, XXX−XXX

Spectroscopic data, FTIR, absorption spectra of receptor **1** on the addition of DNA, DLS histogram, emission spectra of DRHA upon the addition of various ligands, linearity of a sensing mechanism for titration between DRHA and DPA, and concentration of DPA added and found after freeze−thaw cycles and at ambient temperatures (PDF)

AUTHOR INFORMATION

Corresponding Author

*E-mail: nsingh@iitrpr.ac.in.

ORCID

Narinder Singh: 0000-0002-8794-8157

Notes

The authors declare no competing financial interest.

ACKNOWLEDGMENTS

M.V. and N.S. acknowledge the Science & Engineering Research Board (SERB), New Delhi, for National Post Doctoral Fellowship (PDF/2016/000159) and a research project (EMR/2014/000613), respectively.

REFERENCES

(1) Shabani, A.; Marquette, C. A.; Mandeville, R.; Lawrence, M. F. Carbon microarrays for the direct impedimetric detection of Bacillus anthracis using Gamma phages as probes. *Analyst* **2013**, *138*, 1434−1440.

(2) Wang, Y.; Salazar, J. K. Culture-Independent Rapid Detection Methods for Bacterial Pathogens and Toxins in Food Matrices. *Compr. Rev. Food Sci. Food Saf.* **2016**, *15*, 183−205.

(3) Ryu, J.; Lee, E.; Lee, K.; Jang, J. A graphene quantum dots based fluorescent sensor for anthrax biomarker detection and its size dependence. *J. Mater. Chem. B* **2015**, *3*, 4865−4870.

(4) Adams, N. M.; Jackson, S. R.; Haselton, F. R.; Wright, D. W. Design, synthesis, and characterization of nucleic-acidfunctionalized gold surfaces for biomarker detection. *Langmuir* **2012**, *28*, 1068−1082.

(5) Ai, K.; Zhang, B.; Lu, L. Europium-Based Fluorescence Nanoparticle Sensor for Rapid and Ultrasensitive Detection of an Anthrax Biomarker. *Angew. Chem., Int. Ed.* **2009**, *48*, 304−308.

(6) Sivko, G. S.; Stark, G. V.; Tordoff, K. P.; Taylor, K. L.; Glaze, E.; VanRaden, M.; Schiffer, J. M.; Hewitt, J. A.; Quinn, C. P.; Nuzum, E. O. Evaluation of early immune response-survival relationship incynomolgus macaques after Anthrax Vaccine Adsorbed vaccination and Bacillus anthracis spore challenge. *Vaccine* **2016**, *34*, 6518−6528.

(7) Wang, Y.; Zhan, R.; Li, T.; Pu, K.-Y.; Wang, Y.; Tan, Y. C.; Liu, B. Fluorescence and Visual Detection of Single Nucleotide Polymorphism Using Cationic Conjugated Polyelectrolyte. *Langmuir* **2012**, *28*, 889−895.

(8) Plomp, M.; Malkin, A. J. Mapping of proteomic composition on the surfaces of bacillus spores by atomic force microscopy-based immunolabeling. *Langmuir* **2009**, *25*, 403−409.

(9) Lim, D. V.; Simpson, J. M.; Kearns, E. A.; Kramer, M. F. Current and developing technologies for monitoring agents of bioterrorism and biowarfare. *Clin. Microbiol. Rev.* **2005**, *18*, 583−607.

(10) Hugh-Jones, M.; Blackburn, J. The ecology of Bacillus anthracis. *Mol. Aspects Med.* **2009**, *30*, 356−367.

(11) Guimarães, A. P.; Oliveira, A. A.; Da Cunha, E. F. F.; Ramalho, T. C.; França, T. C. C. Analysis of Bacillus anthracis nucleoside hydrolase via in silico docking with inhibitors and molecular dynamics simulation. *J. Mol. Model.* **2011**, *17*, 2939−2951.

(12) Goldman, D. L.; Casadevall, A. Anthrax-associated shock. *Front. Biosci.* **2008**, *13*, 4009−4014.

(13) Irenge, L. M.; Gala, J.-L. Rapid detection methods for Bacillus anthracis in environmental samples: a review. *Appl. Microbiol. Biotechnol.* **2012**, *93*, 1411−1422.

(14) Kim, J.; Yoon, M.-Y. Recent advances in rapid and ultrasensitive biosensors for infectious agents: lesson from Bacillus anthracis diagnostic sensors. *Analyst* **2010**, *135*, 1182−1190.

(15) Seo, Y.; Kim, J.-e.; Jeong, Y.; Lee, K. H.; Hwang, J.; Hong, J.; Park, H.; Choi, J. Engineered nanoconstructs for the multiplexed and sensitive detection of high-risk pathogens. *Nanoscale* **2016**, *8*, 1944−1951.

(16) Gao, R.; Ko, J.; Cha, K.; Jeon, J. H.; Rhie, G.-e.; Choi, J.; deMello, A. J.; Choo, J. Fast and sensitive detection of an anthrax biomarker using SERS-based solenoid microfluidic sensor. *Biosens. Bioelectron.* **2015**, *72*, 230−236.

(17) Okafor, A.; Uddin, M.; Ocando, J. E.; Jespersen, N.; Fan, J.; Wang, E. Spectroscopic Study of Dipicolinic Acid Interaction with Bovine Serum Albumin. *J. Chem. Biochem* **2016**, *4*, 23−46.

(18) Oh, W.-K.; Jeong, Y. S.; Song, J.; Jang, J. Fluorescent Europium-Modified Polymer Nanoparticles for Rapid and Sensitive Anthrax Sensors. Biosens. *Bioelectron* **2011**, *29*, 172−177.

(19) Lepage, D.; Jiménez, A.; Beauvais, J.; Dubowski, J. J. Real-time detection of influenza A virus using semiconductor nanophotonics. *Light: Sci. Appl.* **2013**, *2*, No. e62.

(20) Yilmaz, M. D.; Hsu, S.-H.; Reinhoudt, D. N.; Velders, A. H.; Huskens, J. Ratiometric Fluorescent Detection of an Anthrax Biomarker at Molecular Printboards. *Angew. Chem., Int. Ed.* **2010**, *49*, 5938−5941.

(21) Rieter, W. J.; Taylor, K. M. L.; Lin, W. Surface Modification and Functionalization of Nanoscale Metal-Organic Frameworks for Controlled Release and Luminescence Sensing. *J. Am. Chem. Soc.* **2007**, *129*, 9852−9853.

(22) Bünzli, J.-C. G.; Piguet, C. Lanthanide-Containing Molecular and Supramolecular Polymetallic Functional Assemblies. *Chem. Rev.* **2002**, *102*, 1897−1928.

(23) King, D.; Luna, V.; Cannons, A.; Cattani, J.; Amuso, P. Performance assessment of three commercial assays for direct detection of Bacillus anthracis spores. *J. Clin. Microbiol.* **2003**, *41*, 3454−3455.

(24) Bode, E.; Hurtle, W.; Norwood, D. Real-time PCR assay for a unique chromosomal sequence of B. anthracis. *J. Clin. Microbiol.* **2004**, *42*, 5825−5831.

(25) Son, J. H.; Cho, B.; Hong, S.; Lee, S. H.; Hoxha, O.; Haack, A. J.; Lee, L. P. Ultrafast photonic PCR. *Light: Sci. Appl.* **2015**, *4*, No. e280.

(26) Zhang, Y.; Li, B.; Ma, H.; Zhang, L.; Jiang, H.; Song, H.; Zhang, L.; Luo, Y. A nanoscaled lanthanide metal−organic framework as a colorimetric fluorescence sensor for dipicolinic acid based on modulating energy transfer. *J. Mater. Chem. C* **2016**, *4*, 7294−7301.

(27) Zhang, X.; Young, M. A.; Lyandres, O.; Van Duyne, R. P. Rapid Detection of an Anthrax Biomarker by Surface-Enhanced Raman Spectroscopy. *J. Am. Chem. Soc.* **2005**, *127*, 4484−4489.

(28) Jarvis, R. M.; Goodacre, R. Discrimination of bacteria using surface-enhanced Raman spectroscopy. *Anal. Chem.* **2004**, *76*, 40−47.

(29) Yonzon, C. R.; Stuart, D. A.; Zhang, X.; McFarland, A. D.; Haynes, C. L.; Van Duyne, R. P. Towards advanced chemical and biological nanosensors-An overview. *Talanta* **2005**, *67*, 438−448.

(30) Quang, L. X.; Lim, C.; Seong, G. H.; Choo, J.; Do, K. J.; Yoo, S.-K. A portable surface-enhanced Raman scattering sensor integrated with a lab-on-a-chip for field analysis. *Lab Chip* **2008**, *8*, 2214−2219.

(31) Bantz, K. C.; Meyer, A. F.; Wittenberg, N. J.; Im, H.; Kurtuluş, Ö.; Lee, S. H.; Lindquist, N. C.; Oh, S.-H.; Haynes, C. L. Recent progress in SERS biosensing. *Phys. Chem. Chem. Phys.* **2011**, *13*, 11551−11567.

(32) He, J.; Luo, X.; Chen, S.; Cao, L.; Sun, M.; Yu, Z. Determination of spore concentration in Bacillus thuringiensis through the analysis of dipicolinate by capillary zone electrophoresis. *J. Chromatogr. A* **2003**, *994*, 207−212.

(33) Zhou, Y. X.; Yu, B.; Levon, K. Potentiometric sensor for dipicolinic acid. *Biosens. Bioelectron.* **2005**, *20*, 1851−1855.

(34) Fichtel, J.; Sass, H.; Rullkötter, J. Assessment of spore contamination in pepper by determination of dipicolinic acid with a highly sensitive HPLC approach. *Food Control* **2008**, *19*, 1006−1010.

DOI: 10.1021/acs.langmuir.8b00340
Langmuir XXXX, XXX, XXX−XXX

(35) Havey, C. D.; Basile, F.; Mowry, C.; Voorhees, K. J. Evaluation of a micro fabricated pyrolyzer for the detection of Bacillus anthracis spores. *J. Anal. Appl. Pyrolysis* **2004**, *72*, 55−61.
(36) Bonacchi, S.; Genovese, D.; Juris, R.; Montalti, M.; Prodi, L.; Rampazzo, E.; Sgarzi, M.; Zaccheroni, N. Luminescent chemosensors based on silica nanoparticles. *Top. Curr. Chem.* **2011**, *300*, 93−138.
(37) Kim, H. N.; Guo, Z.; Zhu, W.; Yoon, J.; Tian, H. Recent progress on polymer-based fluorescent and colorimetric chemosensors. *Chem. Soc. Rev.* **2011**, *40*, 79−93.
(38) Fitter, J.; Katranidis, A.; Rosenkranz, T.; Atta, D.; Schlesinger, R.; Büldt, G. Single molecule fluorescence spectroscopy: a tool for protein studies approaching cellular environmental conditions. *Soft Matter* **2011**, *7*, 1254−1259.
(39) Ruedas-Rama, M. J.; Wang, X. J.; Hall, E. A. H. A multi-ion particle sensor. *Chem. Commun.* **2007**, 1544−1546.
(40) Wu, S.; Luo, Y.; Zeng, F.; Chen, J.; Chen, Y.; Tong, Z. Photoreversible Fluorescence Modulation of a Rhodamine Dye by Supramolecular Complexation with Photosensitive Cyclodextrin. *Angew. Chem., Int. Ed.* **2007**, *46*, 7015−7018.
(41) Ma, B.; Zeng, F.; Zheng, F.; Wu, S. Fluorescent detection of an anthrax biomarker based on PVA film. *Analyst* **2011**, *136*, 3649−3655.
(42) Zhou, R.; Zhao, Q.; Liu, K.-K.; Lu, Y.-J.; Dong, L.; Shan, C.-X. Europium-decorated ZnO quantum dots as a fluorescent sensor for the detection of an anthrax biomarker. *J. Mater. Chem. C* **2017**, *5*, 1685−1691.
(43) Rieter, W. J.; Taylor, K. M. L.; Lin, W. Surface Modification and Functionalization of Nanoscale Metal-Organic Frameworks for Controlled Release and Luminescence Sensing. *J. Am. Chem. Soc.* **2007**, *129*, 9852−9853.
(44) Li, M.; Ge, H.; Mirabello, V.; Arrowsmith, R. L.; Kociok-Köhn, G.; Botchway, S. W.; Zhu, W.; Pascu, S. I.; James, T. D. Lysosomal tracking with a cationic naphthalimide using multiphoton fluorescence lifetime imaging microscopy. *Chem. Commun.* **2017**, *53*, 11161−11164.
(45) Shanmugaraju, S.; McAdams, D.; Pancotti, F.; Hawes, C. S.; Veale, E. B.; Kitchen, J. A.; Gunnlaugsson, T. One-pot facile synthesis of 4-amino-1,8-naphthalimide derived Tröger's bases via a nucleophilic displacement approach. *Org. Biomol. Chem.* **2017**, *15*, 7321−7329.
(46) Cao, X.; Meng, L.; Li, Z.; Mao, Y.; Lan, H.; Chen, L.; Fan, Y.; Yi, T. Large Red-Shifted Fluorescent Emission via Intermolecular π-π Stacking in 4-Ethynyl-1,8-naphthalimide-Based Supramolecular Assemblies. *Langmuir* **2014**, *30*, 11753−11760.
(47) Cao, X.; Zhao, N.; Lv, H.; Ding, Q.; Gao, A.; Jing, Q.; Yi, T. Strong Blue Emissive Supramolecular Self-Assembly System Based on Naphthalimide Derivatives and Its Ability of Detection and Removal of 2,4,6-Trinitrophenol. *Langmuir* **2017**, *33*, 7788−7798.
(48) Hua, Q.-X.; Xin, B.; Liu, J.-X.; Zhao, L.-X. .; Xiong, Z.-J.; Chen, T.; Chen, Z.-Q.; Li, C.; Gong, W.-L.; Huang, Z.-L.; Zhu, M.-Q. Bulky 4,6-disubstituted tetraphenylethene-naphthalimide dyad: synthesis, copolymerization, stimuliresponsive fluorescence and cellular imaging. *Faraday Discuss.* **2017**, *196*, 439−454.
(49) Hawes, C. S.; Byrne, K.; Schmitt, W.; Gunnlaugsson, T. Flexible Porous Coordination Polymers from Divergent Photoluminescent 4-Oxo-1,8 naphthalimide Ligands. *Inorg. Chem.* **2016**, *55*, 11570−11582.
(50) Coronado, J. L. G.; Martín, E.; Montero, L. A.; Fierro, J. L. G.; de la Vega, J. M. G. Effects of the 3- and 4-Methoxy and Acetamide Substituents and Solvent Environment on the Electronic Properties of N-Substituted 1,8-Naphthalimide Derivatives. *J. Phys. Chem. A* **2007**, *111*, 9724−9732.
(51) Verma, M.; Luxami, V.; Paul, K. Synthesis, in vitro evaluation and molecular modelling of naphthalimide analogue as anticancer agents. *Eur. J. Med. Chem.* **2013**, *68*, 352−360.
(52) Verma, M.; Luxami, V.; Paul, K. Synthesis, in vitro evaluation and DNA interaction studies of N-allyl naphthalimide analogues as anticancer agents. *RSC Adv.* **2015**, *5*, 41803−41813.
(53) Arjmand, F.; Yousuf, I.; Hadda, T. B.; Toupet, L. Synthesis, crystal structure and antiproliferative activity of Cu (II) nalidixic acid-DACH conjugate: Comparative in vitro DNA/RNA binding profile, cleavage activity and molecular docking studies. *Eur. J. Med. Chem.* **2014**, *81*, 76−88.
(54) Villarreal, W.; Colina-Vegas, L.; Visbal, G.; Corona, O.; Corrêa, R. S.; Ellena, J.; Cominetti, M. R.; Batista, A. A.; Navarro, M. Copper(I)−Phosphine Polypyridyl Complexes: Synthesis, Characterization, DNA/HSA Binding Study, and Antiproliferative Activity. *Inorg. Chem.* **2017**, *56*, 3781−3793.
(55) Silverman, S. K. Pursuing DNA Catalysts for Protein Modification. *Acc. Chem. Res.* **2015**, *48*, 1369−1379.
(56) Rehman, S. U.; Yaseen, Z.; Husain, M. A.; Sarwar, T.; Ishqi, H. M.; Tabish, M. Interaction of 6 Mercaptopurine with Calf Thymus DNA-Deciphering the Binding Mode and Photoinduced DNA Damage. *PLoS One* **2014**, *9*, No. e93913.
(57) Pyle, A. M.; Rehmann, J. P.; Meshoyrer, R.; Kumar, C. V.; Turro, N. J.; et al. Mixed-ligand complexes of ruthenium(II): factors governing binding to DNA. *J. Am. Chem. Soc.* **1989**, *111*, 3051−3058.
(58) Sidhu, J. S.; Singh, A.; Garg, N.; Singh, N. Carbon dot based, naphthalimide coupled fret pair for highly selective ratiometric detection of thioredoxin reductase and cancer screening. *ACS Appl. Mater. Interfaces* **2017**, *9*, 25847−25856.
(59) Diac, A.; Focsan, M.; Socaci, C.; Gabudean, A.-M.; Farcau, C.; Maniu, D.; Vasile, E.; Terec, A.; Veca, M.; Astilean, S. Covalent conjugation of carbon dots with Rhodamine B and assessment of their photophysical properties. *RSC Adv.* **2015**, *5*, 77662−77669.
(60) Kypr, J.; Kejnovska, I.; Renciuk, D.; Vorlickova, M. Circular dichroism and conformational polymorphism of DNA. *Nucleic Acids Res.* **2009**, *37*, 1713−1725.
(61) Nayab, P. S.; Pulaganti, M.; Chitta, S. K.; Rahisuddin. Multispectroscopic and molecular docking studies on the interaction of new phthalimides with calfthymus DNA: In vitro free radical scavenging Activities. *Spectrosc. Lett.* **2016**, *49*, 108−117.
(62) Dorraji, P. S.; Jalali, F. Investigation of the Interaction of Sertraline with Calf Thymus DNA by Spectroscopic Methods. *J. Braz. Chem. Soc.* **2013**, *24*, 939−945.
(63) Mallick, S.; Chandra, F.; Koner, A. L. A ratiometric fluorescent probe for detection of biogenic primary amines with nanomolar sensitivity. *Analyst* **2016**, *141*, 827−831.
(64) Taylor, K. M. L.; Lin, W. Hybrid silica nanoparticles for luminescent spore detection. *J. Mater. Chem.* **2009**, *19*, 6418−6422.
(65) Li, P.; Ang, A. N.; Feng, H.; Sam, F. Y.; Li, J. Rapid detection of an anthrax biomarker based on the recovered fluorescence of carbon dot−Cu(II) systems. *J. Mater. Chem. C* **2017**, *5*, 6962−6972.
(66) Ma, B.; Zeng, F.; Zheng, F.; Wu, S. Fluorescent detection of an anthrax biomarker based on PVA film. *Analyst* **2011**, *136*, 3649−3655.
(67) Veale, E. B.; Gunnlaugsson, T. Bidirectional Photoinduced Electron-Transfer Quenching Is Observed in 4-Amino-1,8-naphthalimide-Based Fluorescent Anion Sensors. *J. Org. Chem.* **2008**, *73*, 8073−8076.
(68) Tan, H.; Ma, C.; Chen, L.; Xu, F.; Chen, S.; Wang, L. Nanoscaled lanthanide/nucleotide coordination polymer for detection of an anthrax biomarker. *Sens. Actuators, B* **2014**, *190*, 621−626.
(69) Xu, J.; Shen, X.; Jia, L.; Zhang, M.; Zhou, T.; Wei, Y. Facile ratiometric fluorapatite nanoprobes for rapid and sensitive bacterial spore biomarker detection. *Biosens. Bioelectron.* **2017**, *87*, 991−997.
(70) Tan, H.; Li, Q.; Ma, C.; Song, Y.; Xu, F.; Chen, S.; Wang, L. Lanthanide-functionalized silver nanoparticles for detection of an anthrax biomarker and test paper fabrication. *J. Nanopart. Res.* **2013**, *16*, 2151−2161.
(71) Chen, H.; Xie, Y.; Kirillov, A. M.; Liu, L.; Yu, M.; Liu, W.; Tang, Y. A ratiometric fluorescent nanoprobe based on terbium functionalized carbon dots for highly sensitive detection of an anthrax biomarker. *Chem. Commun.* **2015**, *51*, 5036−5039.
(72) Donmez, M.; Yilmaz, M. D.; Kilbas, B. Fluorescent detection of dipicolinic acid as a biomarker of bacterial spores using lanthanide-chelated gold nanoparticles. *J. Hazard. Mater.* **2017**, *324*, 593−598.
(73) Zhang, Y.; Li, B.; Ma, H.; Zhang, L.; Zheng, Y. Rapid and facile ratiometric detection of an anthrax biomarker by regulating energy transfer process in bio-metal-organic framework. *Biosens. Bioelectron.* **2016**, *85*, 287−293.

DOI: 10.1021/acs.langmuir.8b00340
Langmuir XXXX, XXX, XXX−XXX